ELSEVIER

Journal of Molecular Catalysis A: Chemical 182–183 (2002) 25–34

JOURNAL OF MOLECULAR CATALYSIS A: CHEMICAL

www.elsevier.com/locate/molcata

Influence of the structure and composition of magnesium phosphate catalysts on the transformation of 2-hexanol

María Ángeles Aramendía, Victoriano Borau, César Jiménez*, José María Marinas, Francisco José Romero[1], Francisco José Urbano

Facultad de Ciencias Edificio C-3, Department of Organic Chemistry, University of Córdoba, Campus de Rabanales, Carretera Nacional IV-A, km 396, E-14014 Cordoba, Spain

Received 2 July 2001; accepted 24 September 2001

Abstract

Various synthetic solids were prepared by precipitation with sodium hydroxide from magnesium chloride or nitrate solutions. The materials thus obtained were characterized in structural terms by using X-ray diffraction, thermogravimetric analysis, EDAX analysis and diffuse reflectance infrared spectroscopy. Their surface properties were determined from N_2 adsorption–desorption isotherms and their chemical properties by using various titrants. Once calcined, the solids were found to consist mainly of sodium–magnesium mixed phosphates; on the other hand, those washed with water were found to contain primarily $Mg_3(PO_4)_2$. The former exhibited a high selectivity towards the formation of hexanone from 2-hexanol; by contrasts, the latter also yielded the corresponding dehydration products (hexenes). The catalytic activity and selectivity results for the reactions leading to the different possible products are related to the structure and composition of the solids.

Keywords: Magnesium phosphates; Sodium–magnesium phosphates; Heterogeneous catalysis; Dehydration–dehydrogenation; 2-Hexanol

1. Introduction

A number of metal phosphates have been used as heterogeneous catalysts for a variety of organic processes in recent years [1,2]. Among them, magnesium orthophosphates have proved useful in various processes of high interest, the results of which have been found to depend on the phosphate's structure and composition. Sokolovskii et al. [3] studied the oxidative transformations of methane on magnesium–phosphorus catalysts and found the increased acidity resulting from an increase in P content to shift the selectivity of the reaction from dimerization to selective oxidation. Ohno and Moffat [4] used alkali and alkaline-earth phosphate catalysts (magnesium orthophosphate included) in the oxidative coupling of methane and found the selectivity towards C_2 and higher hydrocarbons, and also that towards the oxidation products, to depend on the cation radius-to-charge ratio. Sugiyama et al. [5–7] used a commercially available magnesium phosphate in the oxidative dehydrogenation of ethane and oxidative coupling of methane; they showed the presence of chlorinated species on the surface of the solid to enhance its catalytic properties.

Our group has also used various magnesium phosphates in processes including alcohol transformations

* Corresponding author. Tel.: +34-957-218-638; fax: +34-957-212-066.
E-mail addresses: qo1jisac@uco.es (C. Jiménez), qo2rosaf@uco.es (F.J. Romero).
[1] Co-corresponding author. Tel.: +34-957-212-065; fax: +34-957-212-066.

1381-1169/02/$ – see front matter
PII: S1381-1169(01)00463-0

[8], the Meerwein–Ponndorf–Verley reaction [9], diverse condensations in the gas and liquid phase [10,11] and the *N*-alkylation of aniline with methanol [12]. The conversion and selectivity results obtained varied with the particular synthetic procedure followed.

Metal orthophosphates have been used as catalysts for alcohol transformations [1,2] among other processes. The dehydration of the alcohol usually competes with its dehydrogenation, the final proportion of each product depending on the particular catalyst and reaction conditions. Most of these solids exhibit effective dehydrating activity; some, however, have been found to convert secondary alcohols into ketones. The selectivity of a catalyst is dictated by its acid–base and redox properties [13–15], which are acquired during the synthetic process.

The aim of this work was to elucidate the relationship between the particular synthetic procedure used to obtain solids by precipitation with sodium hydroxide from solutions containing magnesium chloride or nitrate and phosphoric acid to the structure, composition and acid–base properties of the resulting solid as reflected in its selectivity in the transformation of 2-hexanol.

2. Experimental

2.1. Synthetic procedure

Solid MgP–N was obtained as follows: a solution containing 81.3 g of $Mg(NO_3)_2{\cdot}6H_2O$ and 14.3 ml of 85% H_3PO_4 in 250 ml of distilled water, placed in an ice bath, was slowly dropped, with stirring, over another containing 3 M NaOH until its pH was lowered to 9. The suspension thus obtained was allowed to stand for 24 h, after which it was filtered and the solid dried. Solid MgP–N-1 was obtained by suspending the previous one in a solution containing 20 g of Na_2CO_3 in 60 ml of distilled water with stirring for 2 h and allowing the suspension to stand for 24 h.

Solid MgP–N-2 was prepared by washing solid MgP–N-1 with isopropyl alcohol. For this purpose, the solid was shaken in the alcohol (5 ml per gram of solid) for 30 min and allowed to stand for 24 h. Solid MgP–N-3 was obtained following a similar procedure except that the starting solid, MgP–N-1, was washed with distilled water (20 ml per gram of catalyst) instead of alcohol.

Solid MgP–Cl was prepared similar to MgP–N but using a different magnesium source. Thus, a solution containing 80 g of $MgCl_2{\cdot}6H_2O$ and 17.8 ml of 85% H_3PO_4 in 250 ml of distilled water, placed in an ice bath, was slowly dropped, with stirring over a 3 M NaOH solution to pH 9. After 24 h, the resulting solid was filtered and air-dried. Such a solid was labeled MgP–Cl and, similar to the previous series, was used to obtain MgP–Cl-1, the washing of which with isopropyl alcohol and distilled water yielded MgP–Cl-2 and MgP–Cl-3, respectively.

All solids were calcined at 773 or 923 K for 3 h and sifted through 200–250 mesh.

2.2. Characterization

X-ray diffraction patterns were recorded on a Siemens D 5000 diffractometer using Cu Kα radiation. Scans were performed over the 2θ range from 2 to 80. Thermogravimetric curves were recorded on a Cahn 2000 electrobalance by heating from 298 to 1123 K at a rate of $10\,K\,min^{-1}$ in a nitrogen atmosphere. Samples were used untreated. The composition of the catalysts was determined by energy-dispersive X-ray analysis (EDAX) on a Jeol JSM-5400 instrument equipped with a Link ISI analyzer and a Pentafet detector (Oxford). Diffuse reflectance IR (DRIFT) spectra for the solids were recorded over the wavenumber range 400–6000 cm^{-1} on a Bomen MB-100 FTIR spectrophotometer. Samples were prepared by mixing 0.14 g of powdered solid with KBr (the blank) in a 15:85 ratio. All samples were preheated at 573 K for 1 h in order to ensure thorough removal of moisture.

2.3. Textural and chemical properties

The specific surface area of each solid was determined using the BET method on a Micromeritics ASAP 2000 analyzer. Acid and basic sites were quantified from retention isotherms for cyclohexylamine ($pK_a = 10.6$) and phenol ($pK_a = 9.9$), respectively, dissolved in cyclohexane. The amount of titrant retained by each solid was measured spectrophotometrically (at 226 and 271.6 nm for cyclohexylamine and phenol, respectively). By using the Langmuir equation, the amount of titrant adsorbed in monolayer

form, X_m, was obtained as a measure of the concentration of acid and basic sites [16].

2.4. Catalytic activity

Reactions were conducted in a glass tubular reactor of 6 mm ID that was fed at the top by means of a SAGE propulsion pump, the flow-rate of which was controlled via a nitrogen flow-meter. The reactor was loaded with 0.175 g of catalyst, over which 1 g of glass beads intended to act as a vaporizing layer was placed. The temperature was controlled via an externally wrapped heating wire that covered the height of both the catalytic bed and the vaporizer, and was connected to a temperature regulator. Evolved gases emerging from the reactor outlet were passed through a condenser onto a collector that allowed liquids to be withdrawn at different times.

No diffusion control mechanism was detected [17], nor was any of the reactor elements found to contribute to the catalytic effect under the reactor's operating conditions in blank runs.

Collected samples were analyzed by gas chromatography on a 60 m × 0.25 mm ID SPB-5 phenylsilicone capillary column, using a linear temperature ramp from 308 to 423 K at 15 K min^{-1}. Products were identified by comparison with standards and their structures confirmed by mass spectrometry.

3. Results and discussion

3.1. Characterization of the solids

Precipitation of the solutions containing magnesium nitrate and phosphoric acid with sodium hydroxide yielded solid MgP–N, the X-ray patterns for which—not shown—exhibited several diffraction bands on a rather ill-defined background. Aging in a sodium carbonate solution gave a more crystalline solid, MgP–N-1, which exhibited the same absorption band as the previous one. Both solids (MgP–N and Mg–P–N-1) possess a complex structure; their spectra include bands for $Mg_3(PO_4)_2{\cdot}8H_2O$ and $Mg(OH)_2$, and also, perhaps, $Mg_3(PO_4)_2{\cdot}22H_2O$ or even $Mg_3(PO_4)_2{\cdot}10H_2O$. The XRD patterns for the solids calcined at 773 and 923 K are quite similar to each other; all include bands for periclase MgO and

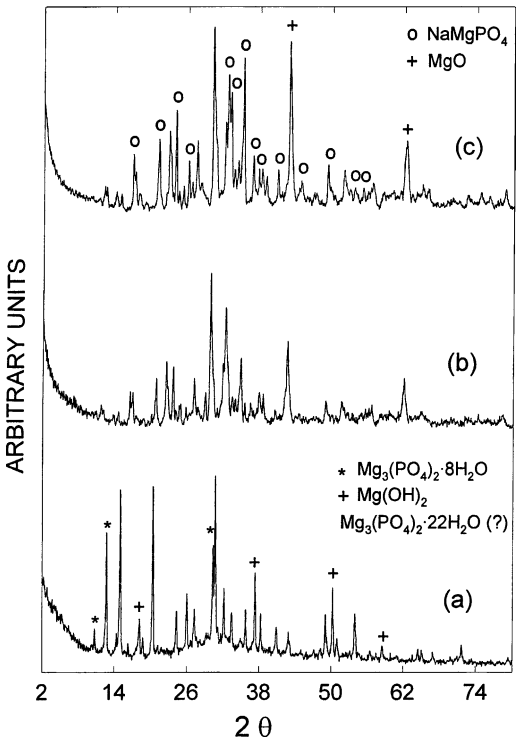

Fig. 1. XRD patterns for solid MgP–N-1: uncalcined (a), calcined at 773 (b) and 923 K (c).

$NaMgPO_4$, in addition to others potentially due to Na_2CO_3 (Fig. 1). There are virtually no signs of the presence of $NaMg_4(PO_4)_3$, which is indeed present in solid MgP–N.

Aging in isopropyl alcohol, which yielded solid MgP–N-2, induced no appreciable changes in the XRD pattern—not shown. By contrast, washing solid MgP–N-1 with distilled water, which yielded solid MgP–N-3, caused a major structural change (Fig. 2). In fact, the solid thus obtained consists of a well-defined $Mg_3(PO_4)_2{\cdot}22H_2O$ structure. Conversion of mixed phosphate into hydrated phosphate by the effect of washing was previously observed by some authors in the transformations of $KMgPO_4{\cdot}H_2O$ and $KMgPO_4{\cdot}6H_2O$ into $Mg_3(PO_4)_2{\cdot}22H_2O$ [18]. Calcination at 773 K yields an amorphous solid that becomes farringtonite $Mg_3(PO_4)_2$. Consequently, solid MgP–N-3 consists mainly of $Mg_3(PO_4)_2$ but may also contain a small amount of MgO. As a result, washing with water avoids the formation of

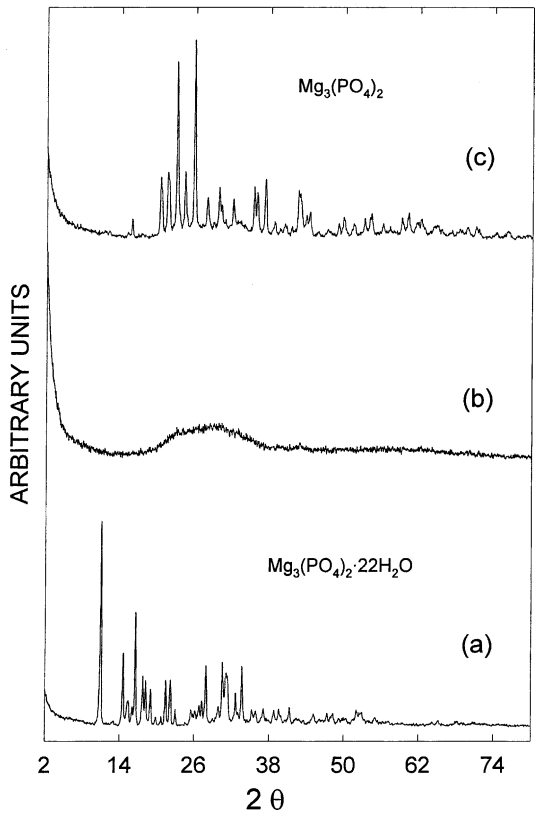

Fig. 2. XRD patterns for solid MgP–N-3: uncalcined (a), calcined at 773 (b) and 923 K (c).

sodium–magnesium mixed phosphates upon calcination. As can be seen from the sequence of XRD patterns obtained at different temperatures, the removal of 22 mol of water per mol of phosphate induces substantial deterioration of the solid structure, which becomes microcrystalline by the effect of a considerable loss of crystallinity (Fig. 2b). A new rise in the calcination temperature yields a crystalline solid of structure $Mg_3(PO_4)_2$, possibly containing traces of periclase MgO.

The solids prepared from magnesium chloride warrant similar comments. Thus, solids MgP–Cl and MgP–Cl-1 exhibit similar XRD patterns—not shown; the latter, however, is somewhat more crystalline. Some bands can be ascribed to species such as $Mg_3(PO_4)_2{\cdot}10H_2O$, $Mg_3(PO_4)_2{\cdot}8H_2O$ and NaCl. However, the species obtained upon calcination exhibit some differences. Thus, solid MgP–Cl loses most of its crystallinity upon calcination at 773 K, so much so that only the bands for NaCl and a few weak bands for MgO can be clearly distinguished. Calcining at 923 K increases its crystallinity; the bands thus obtained are consistent with the presence of farringtonite $Mg_3(PO_4)_2$ and NaCl, and also, perhaps, a small amount of MgO. On the other hand, the XRD patterns for solid MgP–Cl-1 calcined at 773 and 923 K are similar to each other and include bands for $NaMg_4(PO_4)_3$, $NaMgPO_4$, MgO, NaCl and, possibly, Na_2CO_3.

As in the previous case, the solid aged in isopropyl alcohol, MgP–Cl-2, exhibits no difference in its XRD patterns from those for MgP–Cl-1. The solid washed with distilled water, MgP–Cl-3, also undergoes a major structural change: an increase in hydration that yields $Mg_3(PO_4)_2{\cdot}22H_2O$. Calcination at 773 K gives rise to an XRD pattern with an ill-defined background containing weak bands for MgO. Finally, calcination at 923 K yields $Mg_3(PO_4)_2$ and weak bands of MgO.

Table 1 shows the principal phases detected in each solid prior to and after calcination.

Figs. 3 and 4 show the thermogravimetric curves for the solids. All exhibit the same weight loss below 500 K, a loss that, based on reported values [8,19], must correspond to crystallization water from the different phosphates in addition to water potentially adsorbed on their surfaces. The curves for solids

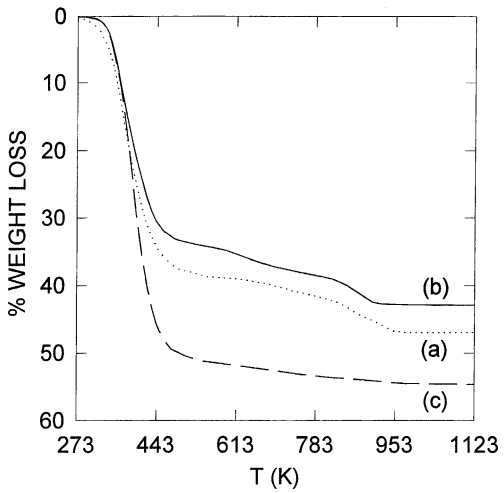

Fig. 3. TGA curves for solids MgP–N-1 (a); MgP–N-2 (b); MgP–N-3 (c).

Table 1
Primary phases found in the solids

Solid	Uncalcined	Calcined
MgP–N	$Mg_3(PO_4)_2{\cdot}8H_2O$, $Mg(OH)_2$, $Mg_3(PO_4)_2{\cdot}22H_2O$ (?), $Mg_3(PO_4)_2{\cdot}10H_2O$ (?)	$NaMgPO_4$, $NaMg_4(PO_4)_3$, MgO
MgP–N-1	Idem MgP–N	$NaMgPO_4$, MgO
MgP–N-2	Idem MgP–N-1	$NaMgPO_4$, MgO
MgP–N-3	$Mg_3(PO_4)_2{\cdot}22H_2O$	$Mg_3(PO_4)_2$[a], MgO (?)
MgP–Cl	$Mg_3(PO_4)_2{\cdot}8H_2O$, $Mg_3(PO_4)_2{\cdot}10H_2O$, NaCl	$Mg_3(PO_4)_2$[a], NaCl, MgO
MgP–Cl-1	Idem MgP–Cl	$NaMgPO_4$, $NaMg_4(PO_4)_3$, MgO, NaCl
MgP–Cl-2	Idem MgP–Cl-1	$NaMgPO_4$, $NaMg_4(PO_4)_3$, MgO, NaCl
MgP–Cl-3	$Mg_3(PO_4)_2{\cdot}22H_2O$	$Mg_3(PO_4)_2$[a], MgO

[a] Amorphous at 773 K.

MgP–N and MgP–Cl are highly similar to those for MgP–N-1 and MgP–Cl-1, respectively. Solids MgP–N, MgP–N-1 and MgP–N-2 exhibit a small weight loss (4–7%) between 750 and 923 K which, however, is absent from the solid washed with distilled water (MgP–N-3). This suggests that the loss may be related to the decomposition of water-soluble species (possibly nitrates formed during the synthetic process). Solid MgP–N-3 is also that exhibiting the greatest total weight loss (54.6%) which can be ascribed to the high water content in its structure [$Mg_3(PO_4)_2{\cdot}22H_2O$].

Table 2 lists the Na/P and Mg/P ratios calculated from the elemental composition of each solid.

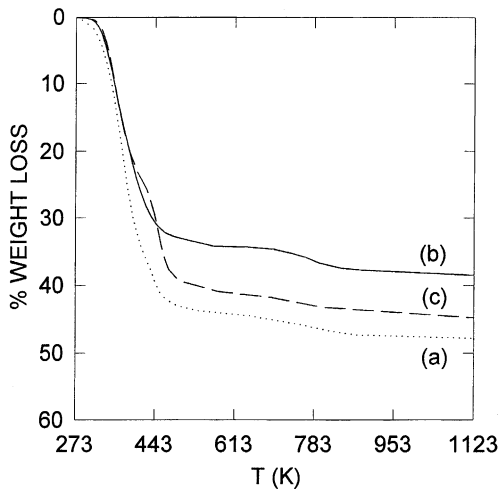

Fig. 4. TGA curves for solids MgP–Cl-1 (a); MgP–Cl-2 (b); MgP–Cl-3 (c).

Overall, the atomic ratios are consistent with the species identified in each solid and also with their solubility in the solvent with which they were treated. A comprehensive description of the effects on each solid is beyond the scope of this paper, so only the most salient findings in this respect are commented on. Specially prominent is the high proportion of sodium in virtually all the solids, consistent with the presence of sodium–magnesium mixed phosphates such as $NaMgPO_4$ and $NaMg_4(PO_4)_3$ (identified by the X-ray technique). This is not the case with solids MgP–N-3 and MgP–Cl-3, which were washed with distilled water and where the sodium content was quite low—particularly in the former; both solids were assigned an $Mg_3(PO_4)_2$ structure. On the other hand, the high Mg/P ratio in all the solids, above the theoretical ratio for pure $Mg_3(PO_4)_2$ (Mg/P = 1.5), suggests the presence of additional magnesium-containing compounds such as MgO. No crystalline $NaMgPO_4$ was identified among the species resulting from washing with water. As noted earlier, this treatment transforms

Table 2
Atom ratios as determined by EDAX for the studied solids, all calcined at 773 K

Solid	Na/P ratio	(Na–Cl)/P ratio	Mg/P ratio
MgP–N	0.79	–	2.08
MgP–N-1	0.74	–	1.78
MgP–N-2	0.94	–	2.09
MgP–N-3	0.15	–	2.45
MgP–Cl	0.86	0.52	2.20
MgP–Cl-1	1.13	0.78	1.98
MgP–Cl-2	1.06	0.85	2.05
MgP–Cl-3	0.21	0.20	2.30

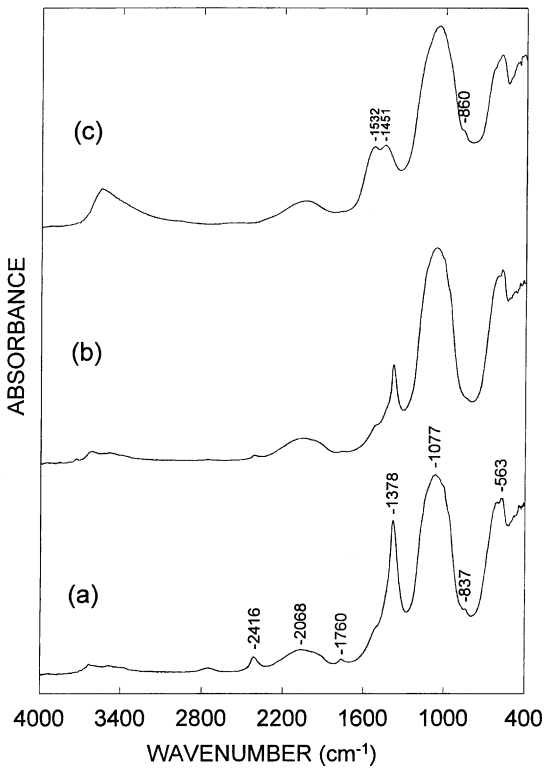

Fig. 5. DRIFT spectra for solids MgP–N-1 (a); MgP–N-2 (b); MgP–N-3 (c).

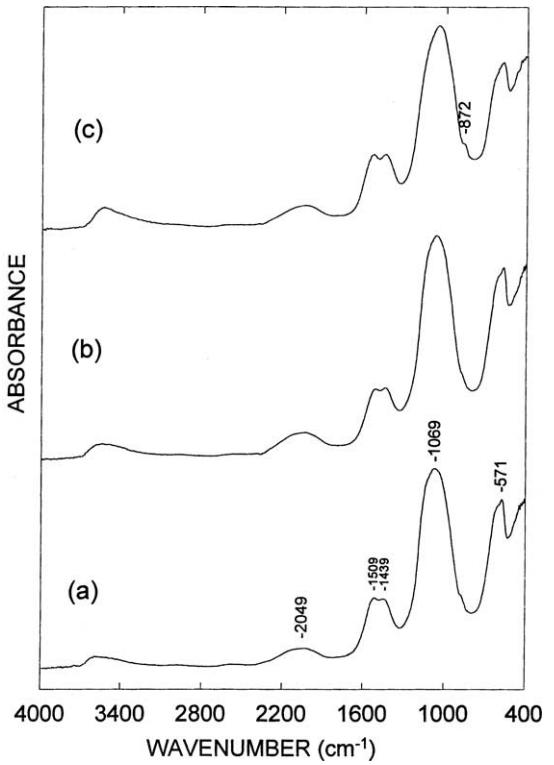

Fig. 6. DRIFT spectra for solids MgP–Cl-1 (a); MgP–Cl-2 (b); MgP–Cl-3 (c).

these hydrated species into $Mg_3(PO_4)_2{\cdot}22H_2O$ [18], which subsequently yields soluble sodium phosphates that are removed by the washing water and result in substantial losses of sodium and phosphorus. Magnesium must remain both as phosphate and as residual $Mg(OH)_2$, which would be highly disperse and increase the Mg/P ratio to levels higher than even the theoretical value. On the other hand, some phosphates are partially soluble in alcohols, depending on the particular temperature and treatment time. The presence of other species such as $NaMg_4(PO_4)_3$ on the solid surface may also account for these results—to an extent that cannot be quantified.

Figs. 5 and 6 show the DRIFT spectra for the solids following calcination at 773 K. All the spectra exhibit a broad strong band between 1000 and 1100 cm^{-1} that is present in the spectra for all phosphates of generic formula $M_3{}^{+}PO_4{}^{3-}$ [20–22]. The band at 1017 cm^{-1} can be assigned to ν_3 (antisymmetric stretching) and that at 567 cm^{-1} to a ν_4 (out-of-plane bending) vibration of phosphate [21]. The region from 1600 to 2300 cm^{-1} contains a series of broad, weak bands that can be assigned to O=P–OH groups the frequency of which has been decreased by hydrogen bonding.

The region from 3000 to 3800 cm^{-1} contains a broad band due to O–H vibrations. The band is stronger in solids MgP–N-3 and MgP–Cl-3 (i.e. those washed with water), which suggests a higher degree of hydroxylation. On the other hand, the presence of a substantial proportion of MgO in the solids would have resulted in a band at 3739 cm^{-1}, typically assigned to vibrations of hydroxyl groups of the Mg–OH type located at crystallite edges and corners [23–25]; no such band was found for any of the solids, however.

Solids MgP–N, MgP–N-1 and MgP–N-2 exhibit an additional, quite strong band at 1378 cm^{-1} plus a weaker one at 837 cm^{-1} that correspond to the ν_3

(antisymmetric stretching) and ν_2 (out-of-plane bending) vibrations, respectively, of nitrate ion [21]. As can be seen, these bands are absent from the spectrum for solid MgP–N-3, which indicates that residual nitrates disappear by solubilization during washing with distilled water. Both this solid and those obtained from magnesium chloride exhibit two bands between 1400 and 1550 cm^{-1}, and one other between 860 and 880 cm^{-1}, which correspond to the ν_3 (antisymmetric stretching) and ν_2 (out-of-plane bending) vibrations of carbonates, respectively [8,21,26]. This indicates the formation of surface carbonates on these solids as a result of using either sodium hydroxide as precipitant during the synthetic process or CO_2 being adsorbed during calcination in the air.

3.2. Textural and chemical properties

Table 3 shows the specific surface areas, and the populations of acid and basic sites of the solids. All exhibit type IV N_2 adsorption isotherms, which are typical of mesoporous solids as per the BDDT classification [27]; also, all exhibit a type A (or H_1) hysteresis cycle as per the De Boer classification [28,29], often associated with porous materials consisting of agglomerates. In general, the solids possess a low specific surface area and a porous network consisting of large pores of widely variable sizes in the range from mesoporous to macroporous (the average pore size is 200–400 Å).

The solids obtained from magnesium chloride (e.g. MgP–Cl and MgP–Cl-1) seem to possess slightly higher surface areas than those prepared from magnesium nitrate (MgP–N and MgP–N-1). Washing with isopropyl alcohol seemingly causes a slight increase in area, because of the low surface area of the starting solid, however, the increase is insubstantial, particularly with relation to changes in other types of solid such as $AlPO_4$, the thermal treatment of which has been found to result in an area loss of 40–70% in materials exposed to water but only 10–20% in others exposed to isopropyl alcohol [30]. However, the treatment most significantly altering the surface area of the studied phosphates is washing with water. Thus, solids MgP–Cl-3 and MgP–N-3 possess an area of 23 and 33 $m^2\,g^{-1}$, respectively. In addition to the removal of soluble species (detected by TGA, DRIFT spectroscopy or EDAX analysis), this treatment causes both structural changes (primarily the formation of $Mg_3(PO_4)_2{\cdot}22H_2O$ as observed by XRD spectroscopy) and surface changes such as the increased degree of hydroxylation observed by DRIFT spectroscopy.

Table 3 also shows the populations of acid and basic sites in the solids. Those that were washed with water exhibit not only structural and morphological changes that alter their crystallinity and composition, but also an increased surface area and degree of hydroxylation, which result in a marked increase in the number of acid and basic sites. A similar though weaker effect also arises from the treatment with isopropyl alcohol. As expected, these washing-induced changes are more marked in the MgP–N series, where the solids contain greater amounts of $NaMgPO_4$—removal of which by washing with water has such dramatic consequences. The population of acid sites is larger than that of basic sites in all solids.

Table 3
Textural and chemical properties of the studied solids, all calcined at 773 K

Solid	S_{BET} ($m^2\,g^{-1}$)	Acid sites ($\mu mol\,g^{-1}$)	Basic sites ($\mu mol\,g^{-1}$)
MgP–N	6	18	13
MgP–N-1	7	–	8
MgP–N-2	8	14	8
MgP–N-3	33	70	38
MgP–Cl	9	23	11
MgP–Cl-1	12	23	14
MgP–Cl-2	16	32	14
MgP–Cl-3	23	51	25

3.3. Catalytic activity

Table 4 shows the activity and selectivity in the transformation of 2-hexanol in the gas phase using the studied solids (previously calcined at 773 K). The main reactions promoted by these catalysts are dehydration of the alcohol to the corresponding alkenes and dehydrogenation to the carbonyl derivative (2-hexanone).

All solids except those that were washed with water proved highly selective towards the dehydrogenation reaction, so 2-hexanone was invariably the major product. In other words, all the solids that were assumed to contain sodium–magnesium phosphates favored dehydrogenation over dehydration.

Table 4
Overall conversion (mol%) and selectivity towards hexenes (HENES) and 2-hexanone (HONE) in the transformation of 2-hexanol over the studied solids, all calcined at 773 K[a]

Solid	X_T (mol%)	S_{HENES}	S_{HONE}
MgP–N	14.0	0.056	0.899
MgP–N-1	10.7	–	0.980
MgP–N-2	26.5	0.022	0.917
MgP–N-3	38.3	0.663	0.310
MgP–Cl	12.7	0.209	0.729
MgP–Cl-1	6.4	0.127	0.809
MgP–Cl-2	26.9	0.113	0.835
MgP–Cl-3	29.3	0.287	0.667

[a] Reactions conditions: N_2 flow rate, 40 ml min^{-1}; catalyst weight, 0.175 g; feed rate, 3.88 ml h^{-1}; T_{reac} = 773 K; t_{react} = 120 min.

The dehydration–dehydrogenation of alcohols is a model reaction for studying the acid–base properties of solid catalysts [31]. Some authors have ascribed the dehydrating ability of a solid to its acidity [32] and its dehydrogenating ability to its basicity [33]; others, however, believe that the dehydrogenation reaction is catalyzed by both types of site (acid and basic) via a concerted mechanism [34]. Based on this assumption, our phosphates must be essentially basic solids. As noted earlier, however, the population of acid sites was larger than that of basic sites, so the sites titrated by cyclohexylamine or phenol are not strictly the same as those responsible for catalytic activity. Consequently, measurements of this type in solids containing few sites and of such a low strength—the highest acid strength estimated for magnesium orthophosphate is $H_0 = +4.8$ [35]—must be used with caution.

Washing the solids with water also alters the selectivity of the reaction: it increases the yield of hexenes—which are the major products with solid MgP–N-3. In fact, these solids possess a larger population of acid sites—but also of basic ones—than the rest. Although, they behave like solids with acid–base properties, the ratio of titrated acid-to-basic sites is about 2 and similar to those for the other solids. In addition, the density of acid sites, unlike their number, is similar (2 μmol m^{-2}) for all the solids irrespective of the selectivity exhibited in the reaction. On the other hand, cyclohexylamine and phenol might be adsorbed at acid–base pairs. All this suggests that the activity and selectivity in the transformation of the alcohol are influenced by the structure of the surface sites.

Tada [36] ascribed the presence of basic sites in various alkali metal phosphates to the presence of P–O–M sites (M = Li, Na, K). If the metal atom is a strong enough electron donor, then the oxygen atoms in the P–O–M sequences will possess a high electron density and hence basic character. Consequently, P–O–Na sites must be those responsible for the dehydrogenating activity of sodium–magnesium mixed phosphates (those in the solids not washed with water). Such solids (MgP–N-3 and MgP–Cl-3) possess an $Mg_3(PO_4)_2$ structure to a greater or lesser extent and hence Brönsted sites of the P–O–H type [37]. In addition, solid MgP–N-3, which possesses a purer $Mg_3(PO_4)_2$ structure, and lower sodium and MgO contents in addition to an increased surface area and site population, exhibits the highest selectivity towards the dehydration reaction.

In order to discard the influence of impurities present in the solids, only in some cases could the presence of sodium–magnesium mixed phosphates be ascertained (from the XRD patterns); alternative solids of well-defined structure and composition were synthesized so as to establish the contribution of the different species to the catalytic activity. Table 5 summarizes the results [25,38], which confirm our hypothesis that the main agents responsible for the dehydrogenating activity and selectivity of the studied phosphates are sodium–magnesium mixed phosphates and hence the basic sites of the P–O–Na type can act in isolation or in a concerted manner with acid surface sites. As can be seen, the presence of MgO by itself cannot account for the high selectivity towards 2-hexanone as dehydration predominates even

Table 5
Overall conversion (mol%) and selectivity towards hexenes (HENES) and 2-hexanone (HONE) in the transformation of 2-hexanol over different solids[a]

Solid	X_T (mol%)	S_{HENES}	S_{HONE}
$Mg_3(PO_4)_2$	97.1	0.982	0.017
75% $Mg_3(PO_4)_2$/25% MgO	100	0.972	0.028
50% $Mg_3(PO_4)_2$/50% MgO	82.7	0.805	0.186
MgO	41.3	0.149	0.694
5 wt.% $Na_2CO_3/Mg_3(PO_4)_2$	40.7	0.804	0.190
10 wt.% $Na_2CO_3/Mg_3(PO_4)_2$	29.3	0.531	0.463

[a] Reactions conditions: N_2 flow rate, 40 ml min^{-1}; catalyst weight, 0.175 g; feed rate, 3.88 ml h^{-1}; T_{reac} = 773 K; t_{react} = 120 min.

when the $Mg_3(PO_4)_2$/MgO ratio equals unity—the boundary case for the elemental composition found in the studied solids (Table 2). As can be seen from Table 5, potential sodium carbonate impurities might have some effect as alkaline carbonates are known to act as heterogeneous basic catalysts in Knoevenagel reactions [39]. Although, they might be present, in fairly low proportions in any case.

In summary, the presence of basic sites in the studied phosphates, which is indispensable for the dehydrogenation of 2-hexanol to 2-hexanone, can largely be ascribed to the presence of sodium–magnesium phosphates, even though there might indeed be some additional slight contribution from other species (e.g. MgO) present in the solids.

4. Conclusions

A series of magnesium orthophosphate solids with differential composition and textural and acid–base properties was synthesized following various procedures. The solids were found to exhibit excellent dehydrating and dehydrogenating activity in the transformation of gaseous 2-hexanol, the selectivity of each individual solid in the process depending on its textural and morphological features. The dehydrogenating activity of the catalysts can be ascribed to the presence of $NaMgPO_4$, and also, perhaps, to that of MgO formed during the synthetic process. The presence of this mixed phosphate is also related to the basic sites in the solid. Those catalysts that were washed with water underwent major structural changes resulting from the disappearance of water-soluble species. The water also had a substantial effect on the degree of surface hydroxylation of the solids and hence on the population of acid and basic sites which in turn altered the selectivity. When washing resulted in the disappearance of $NaMgPO_4$ after calcination, the selectivity towards 2-hexanone was decreased; on the other hand, when the treatment increased with the number of acid sites, the selectivity towards hexenes was boosted.

Acknowledgements

The authors would like to thank Spain's Dirección General de Investigación, Ministerio de Ciencia y Tecnología, for funding this research within the framework of Project BQU2001-2605, and Junta de Andalucía for additional financial support.

References

[1] J.B. Moffat, Catal. Rev. Sci. Eng. 18 (1978) 199.
[2] J.B. Moffat, in: M. Grayson, E.J. Griffith (Eds.), Topics in Phosphorus Chemistry, Vol. 10, Wiley, New York, 1980, p. 285.
[3] V.D. Sokolovskii, Z.G. Osipova, L.M. Plyasova, A.A. Davydov, A.A. Budneva, Appl. Catal. A 101 (1993) 15.
[4] T. Ohno, J.B. Moffat, Catal. Lett. 9 (1991) 23.
[5] S. Sugiyama, J.B. Moffat, Energy Fuels 8 (1994) 463.
[6] S. Sugiyama, K. Satomi, N. Kondo, N. Shigemoto, H. Hayashi, J.B. Moffat, J. Mol. Catal. 93 (1994) 53.
[7] S. Sugiyama, N. Kondo, K. Satomi, H. Hayashi, J.B. Moffat, J. Mol. Catal. A 95 (1995) 35.
[8] M.A. Aramendía, V. Borau, C. Jiménez, J.M. Marinas, F.J. Romero, J.A. Navío, J. Barrios, J. Catal. 157 (1995) 97.
[9] M.A. Aramendía, V. Borau, C. Jiménez, J.M. Marinas, F.J. Romero, Catal. Lett. 58 (1999) 53.
[10] M.A. Aramendía, V. Borau, C. Jiménez, J.M. Marinas, F.J. Romero, J. Catal. 183 (1999) 119.
[11] M.A. Aramendía, V. Borau, C. Jiménez, J.M. Marinas, F.J. Romero, React. Kinet. Catal. Lett. 69 (2000) 311.
[12] M.A. Aramendía, V. Borau, C. Jiménez, J.M. Marinas, F.J. Romero, Appl. Catal. A 183 (1999) 73.
[13] K. Tanabe, M. Misono, I. Ono, N. Hattori, Stud. Surf. Sci. Catal. 51 (1989).
[14] M. Ai, J. Catal. 49 (1977) 305.
[15] A. Ouqour, G. Coudurier, J.C. Vedrine, J. Chem. Soc., Faraday Trans. 89 (1993) 3151.
[16] M.A. Aramendía, V. Borau, C. Jiménez, J.M. Marinas, F. Rodero, Colloids Surf. 12 (1984) 227.
[17] R.M. Koros, E.J. Novak, Chem. Eng. Sci. 22 (1967) 470.
[18] A.W. Taylor, A.W. Frazier, E.L. Gurney, Trans. Faraday Soc. 59 (1963) 1580.
[19] Y. Bakaev, A.V. Dzisco, L.G. Karakchiev, E.M. Moroz, G.N. Kustova, L.T. Tsikova, Kinet. Katal. 5 (1974) 1275.
[20] L.J. Bellamy, The Infra-red Spectra of Complex Molecules, Chapman & Hall, London, 1975.
[21] K. Nakamoto, Infrared and Raman Spectra of Inorganic and Coordination Compounds, 4th Edition, Wiley, New York, 1986.
[22] E.D. Bergmann, U.Z. Littauer, S. Pinchas, J. Chem. Soc. (1952) 847.
[23] P.J. Anderson, R.F. Horlock, J.F. Oliver, J. Chem. Soc., Faraday Trans. 61 (1965) 2754.
[24] T. López, I. García-Cruz, R. Gómez, Mater. Chem. Phys. 36 (1994) 222.
[25] M.A. Aramendía, V. Borau, C. Jiménez, J.M. Marinas, F.J. Romero, J. Colloid Interf. Sci. 219 (1999) 201.
[26] K. Kandori, A. Yasukawa, T. Ishikawa, Chem. Mater. 7 (1995) 26.

[27] S. Brunauer, L.S. Deming, W.S. Deming, E. Teller, J. Am. Chem. Soc. 62 (1940) 1723.
[28] J.H. De Boer, The Structure and Properties of Porous Materials, Butterworths, London, 1958.
[29] K.S.W. Sing, D.H. Everest, R.A.W. Haul, L. Moscou, R.A. Pierotti, J. Rouquérol, T. Siemieniewska, Pure Appl. Chem. 57 (1985) 603.
[30] K. Kearby, Proceedings of the Second International Catalysis Congress, Paris, 1960, p. 2567.
[31] M.A. Aramendía, V. Borau, C. Jiménez, J.M. Marinas, A. Porras, F.J. Urbano, J. Catal. 161 (1996) 829.
[32] F. Figueras-Rocca, L. Mourgues, Y. Trambouze, J. Catal. 14 (1969) 107.
[33] Y. Matsumura, K. Hashimoto, S. Yoshida, J. Catal. 117 (1989) 135.
[34] A. Gervasini, A. Auroux, J. Catal. 131 (1991) 190.
[35] T. Imanaka, Y. Okamoto, S. Teranishi, Bull. Chem. Soc. Jpn. 45 (1972) 1353.
[36] A. Tada, Bull. Chem. Soc. Jpn. 45 (1975) 1391.
[37] M.A. Aramendía, V. Borau, C. Jiménez, J.M. Marinas, F.J. Romero, J.R. Ruiz, J. Solid State Chem. 135 (1998) 96.
[38] M.A. Aramendía, V. Borau, C. Jiménez, J.M. Marinas, F.J. Romero, Colloids Surf. A 170 (2000) 51.
[39] M.A. Aramendía, V. Borau, C. Jiménez, J.M. Marinas, F.J. Romero, Chem. Lett. (1995) 279.